

N O T I C E

THIS DOCUMENT HAS BEEN REPRODUCED FROM
MICROFICHE. ALTHOUGH IT IS RECOGNIZED THAT
CERTAIN PORTIONS ARE ILLEGIBLE, IT IS BEING RELEASED
IN THE INTEREST OF MAKING AVAILABLE AS MUCH
INFORMATION AS POSSIBLE

NASA Technical Memorandum 81405

FRACTURE MODES OF HIGH MODULUS
GRAPHITE/EPOXY ANGLEPLIED LAMINATES
SUBJECTED TO OFF-AXIS TENSILE LOADS

(NASA-TM-81405) FRACTURE MODES OF HIGH
MODULUS GRAPHITE/EPOXY ANGLEPLIED LAMINATES
SUBJECTED TO OFF-AXIS TENSILE LOADS (NASA)
22 p HC A02/ME A01

N80-16102

CSCL 11D

Unclass

G3/24

47034

J. H. Sinclair
Lewis Research Center
Cleveland, Ohio

Prepared for the
Thirty-fifth Annual Conference of the
Reinforced Plastics/Composites Institute
sponsored by the Society of Plastics Industries
New Orleans, Louisiana, February 4-8, 1980

FRACTURE MODES OF HIGH MODULUS GRAPHITE/EPOXY ANGLEPLIED
LAMINATES SUBJECTED TO OFF-AXIS TENSILE LOADS

by J. H. Sinclair

NASA Lewis Research Center
Cleveland, Ohio 44135

ABSTRACT

Angleplied laminates of high modulus graphite fiber/epoxy were studied in several ply configurations at various tensile loading angles to the zero ply direction in order to determine the effects of ply orientations on tensile properties, fracture modes, and fracture surface characteristics of the various plies. It was found that fracture modes in the plies of angleplied laminates can be characterized by scanning electron microscope observation. The characteristics for a given fracture mode are similar to those for the same fracture mode in unidirectional specimens. However, no simple load angle range can be associated with a given fracture mode.

INTRODUCTION

E-319

Fracture surface characteristics and fracture modes have been studied and reported for uniaxial HMG/E laminates subjected to off-axis tensile tests. In Reference 1 criteria (based on examination of fractured tensile specimens by use of a scanning electron microscope (SEM)) were established which can be used to characterize fracture surfaces from such a laminate with respect to a predominant "single-stress" fracture mode. In Reference 2 criteria were developed for identifying, characterizing, and quantifying fracture modes in the same types of laminates. It was found that off-axis composites fail by three predominant fracture modes which produce unique fracture surface characteristics. The stress dominating each fracture mode and the load angle range of its dominance can be identified. The work reported herein is an extension of the above mentioned work as applied to angleplied laminates. The objective was to test angleplied laminates to investigate fracture surface characteristics and associated tensile properties and to establish correlation, if any, between fracture surface characteristics of angleplied laminates and those from the off-axis (uniaxial) laminates previously reported.

Angleplied laminates of high modulus graphite fiber/epoxy were studied in four configurations $[0_2 \pm 15]_s$, $[0_2 \pm 30]_s$, $[0_2 \pm 45]_s$, and $[0_2, 90_2]_s$ to determine the effects of ply orientations on tensile properties, fracture modes and fracture surface characteristics of the various plies. Specimens from each laminate were tested in tension at five angles (0° , 10° , 30° , 45° , and 90°) to the zero ply direction.

SPECIMEN FABRICATION, PREPARATION, INSTRUMENTATION AND TESTING

The laminates, consisting of eight plies of Modmor-I graphite fibers oriented as required in a matrix of ERLA-4617 epoxy resin cured with meta-

phenylene diamine (MPDA), were fabricated by a commercial vendor. These composites will be referred to as Mod I/E hereinafter. The vendor used the following curing procedure. The laminates were heated from room temperature to 121° C (250° F) under a partial vacuum of approximately 2 newtons per square centimeter (N/cm²) (3 psi) and held for 40 minutes at this temperature. They were then heated to 177° C (350° F) under an autoclave pressure of 34.5 N/cm² (50 psi) and held for 2 hours. Pressure was maintained until they had cooled to 49° C (120° F).

Tensile specimens, laid out at the desired load angles on the laminate plates (Fig. 1), were cut slightly over-width by a 0.061-centimeter (0.024-in.) thick diamond wheel mounted on a surface grinder. Stacks of specimens, so cut, were placed on edge and dressed down to the required 1.27-centimeter (0.500-in.) width by a diamond wheel. Specimen ends were reinforced with adhesively bonded fiber glass tabs. The final dimensions of the specimen were about 25.4 centimeters (10 in.) long, 1.27 centimeters (0.5 in.) wide, and about 0.142 centimeter (0.056 in.) thick.

Tensile specimens were instrumented with either 2 or 5 120-ohm, 60° delta-rosette strain gages arranged as shown in Figure 2. The test specimens were loaded to fracture using a hydraulically actuated universal testing machine. Loading was incremental to facilitate periodic recording of strain gage data.

Fractured surfaces of selected tensile specimens were observed by means of a scanning electron microscope (SEM), and typical photomicrographs were made to illustrate fracture modes.

Segments of tested laminates containing the fracture surfaces of interest were cut (while carefully preserving fracture surfaces) from each specimen and cemented (on edge with fracture surface up) to aluminum mounts. In order to facilitate observation by SEM, the specimens were made electrically conductive by coating them with a gold-palladium film, approximately 200 Å (20 nm) thick, which was applied by vapor deposition in a vacuum evaporator. They were then studied and photographed with a JUL-JSM-2 scanning electron microscope.

Only one specimen was tested at each orientation so that fabrication-variable effects on the measured data would be minimized. The number of specimens that could be made from a single laminate was determined by laminate size, which in this case was limited to a square, 30.5 centimeters (12.0 in.) on a side (Fig. 1). Past experience has shown that the effects of orientation are more readily identified by testing specimens from the same laminate at several orientations rather than by testing replicates (from the same laminate) at a given orientation and then selecting specimens from different laminates for the different orientations.

RESULTS AND DISCUSSION

The experimental results consist of stress-strain data (center gages), selected plots, fracture stresses and strains, and SEM photographs of fracture surfaces.

Stress-Strain Data

The strain-gage data reduction program (SGDR) (Ref. 3) was used to generate stress-strain curves from the incremental loads and corresponding data recorded from strain gages. Three types of curves were generated: structural axes stress σ_{cyy} , Poisson's strains ν_{cyy} , and the coupled shear strains ϵ_{cxy} as functions of axial strains ϵ_{cyy} . Stress strain curves for specimens from four of the angleplied laminates tested at four loading angle (0° , 10° , 45° , and 90°) are presented here (Figs. 3, 4, 5, and 6). The 0° and 90° curves were selected because longitudinal and transverse tensile data are necessary to characterize a fiber laminate. Ten degree off-axis data, which are useful for intralaminar shear characterization of uniaxial composites, are presented for comparative purposes, and the 45° load angle was selected because this test angle gives large angle ply relative rotations. Poisson's strain curves and coupled shear strain curves are shown for 10° off-axis specimens only (Figs. 7 and 8). The stress-strain curves (Figs. 3, 4, 5, and 6) are essentially linear.

The fracture stresses for these specimens range from 28 to 476 MPa (4 to 69 ksi) and the fracture strains from 0.2 to 0.5 percent. The Poisson's strain curves (Fig. 7) for the specimens tested at 10° off-axis are linear and the Poisson's strains range from about -0.1 to 0.2 percent. The coupled shear strain curves (Fig. 8) are nearly linear except for the laminate $[0_2 \pm 45]_s$ which appears to be erratic.

Fracture stresses, strains, moduli, Poisson's ratios and coupling coefficients for all specimens reported herein are presented in Table I.

In general, fracture stresses decrease progressively as load angles increase and the fibers approach transverse orientation until we consider the $[0_2, 90_2]_s$ laminate. For that case, once the load angle reaches 45° , the transverse plies begin to approach 0° with further increase of the load angle toward 90° . In this case (although all of these data are not presented here) there is a progressive increase in fracture stress until at 90° off-axis the composite, as expected, is nearly as strong as it was at 0° (Table I).

Fracture strains for all specimens range from about 0.2 to 0.5 percent as shown in Table I, while the moduli, lie between 7 and 214 GPa (1 and 31 MSI). Moduli decrease with increasing load angles in a manner similar to fracture stresses.

The Poisson's ratios for the specimens discussed in this report are also presented in Table I. They lie between -0.3 and 0.9. The shear-strain-normal-strain coupling coefficients for the same group of specimens are summarized in the last four columns of Table I.

SEM Results

In earlier papers fracture modes of off-axis tensile specimens of high modulus graphite-fiber/epoxy resin matrix (MOD I/E) were associated with approximate load angle ranges (References 1, 2, 4, and 5). These fracture modes could be identified by the fracture surface characteristics as observed in SEM

photomicrographs. The fracture modes identified were: (1) longitudinal tensile fracture -the fracture surface was irregular and tiered and was characterized by dominant fiber fracture, fiber pull-out with fiber surfaces clear of matrix residue, and some matrix lacerations on inter-fiber surfaces connecting two different tier levels; (2) intralaminar shear stress fracture -the fracture surface was characterized by a regular or level surface with extensive matrix lacerations; (3) transverse tensile fracture -the fracture surface was characterized by a regular surface with extensive matrix cleavage; and (4) mixed mode (transverse tensile and intralaminar shear)-the fracture surface was level (regular) with areas of both resin lacerations and resin cleavage.

A plot from Reference 5 that can be used to identify the single-stress influence on off-axis tensile fracture is reproduced in Figure 9. It shows fracture stresses normalized with their respective uniaxial strengths. The approximate load angle ranges where the various stresses predominate can readily be seen in the figure.

Fracture surfaces of the angleplied laminates were studied by SEM to determine their fracture surfaces characteristics. A one-to-one correspondence with uniaxial data would not necessarily be expected because of possible interactions among contiguous plies with differing fiber orientations. Figure 10 shows the fiber orientations in the plies of selected laminates studied at some of the load angles. Ply stress calculations made by use of laminate analysis but not included in this report are also used to help explain some of the results. These calculations are analogous to those described in Reference 6.

The laminate $[0_2 \pm 15]_s$ tested along the zero ply direction had fibers of 0° , 15° , and -15° in the various plies. The fracture surface of a ply oriented at 15° with respect to the specimen tensile axis (hereafter referred to as a 15° off-axis ply) is shown in Figure 11. The fracture of this ply was a secondary fracture. Ply stress calculations showed that the zero degree plies failed first in longitudinal tension. Once the zero plies fractured, nothing remained to support the load except 15° off-axis plies which then failed. Reference to Figure 9 indicates that a ply with this orientation should fracture predominantly by intralaminar shear. The lacerated resin matrix associated with this mode of fracture is seen in the SEM photomicrograph.

SEM results were also available for the 30° off-axis tensile specimen from the same $[0_2 \pm 15]_s$ laminate. The fibers in the 0° , $+0$ and -0 plies were oriented at 30° , 45° and 15° respectively with respect to the specimen tensile axis. SEM photomicrographs of fractures in a 0° ply, $+0$ ply, -0 ply, and a general view are pictured in figure 12(a), (b), (c), and (d) respectively. The zero plies, oriented at 30° off-axis in this specimen, (fig. 12(a)) show the mixed mode characteristics as expected. There is extensive matrix cleavage typical of transverse tensile fractures but also matrix lacerations are beginning to appear. The lacerations indicate intralaminar shear fracture. The $+0$ ply oriented at 45° , Figure 12(b), has fiber surfaces free of matrix residue and some matrix cleavage both of which are typical of transverse tensile fracture. The -0 plies, were oriented 15° off-axis in the tensile specimen. Intralaminar shear would be the expected fracture mode for a ply so oriented (Fig. 9). The fracture, Figure 12(c) has the

REPRODUCIBILITY OF THE
ORIGINAL PAGE IS POOR

5

severely lacerated resin matrix and clean fiber surfaces associated with intralaminar shear stress fractures. Figure 12(d) contains enough of the fracture surface of the specimen to include areas of all three ply orientations. Note that the plies containing fibers oriented at different angles are easily distinguishable.

A specimen from laminate $[0_2 \pm 30]_s$ was tested at 10° off-axis. Fracture surfaces are shown in Figure 13. Its 0° , $+0^\circ$ and -0° plies were oriented at 10° , 40° , and -20° with respect to the specimen tensile axis respectively. The predominant fracture stress in a uniaxial composite tested at 10° off-axis would be expected to be intralaminar shear (Figure 9). However, in the laminate $[0_2 \pm 30]_s$ tested at 10° off-axis the zero plies (now oriented at 10° off-axis) are restrained by the -0° plies (now at -20°), causing the 0° plies to fail by longitudinal tensile stresses. This illustrates a change in the predominant fracture stress due to the interaction among adjacent plies with differing fiber orientations. Figure 13(a) shows the fractured surface. The fractured plies exhibited irregular, tiered fracture surfaces. These surfaces are visible at the left edge of the SEM photomicrograph. Also, some matrix cleavage and some matrix lacerations on interfiber surfaces connecting different tier levels (characteristics associated with fiber tensile fracture) are apparent. Once these most nearly longitudinal fibers in the zero plies were broken, the -0° plies probably failed dynamically. They appear to have failed by transverse tension (Fig. 13(b)). These plies would normally be in the transition region where both intralaminar shear and transverse tension would contribute to fracture (Fig. 9); they would, therefore, be expected to show some lacerated resin associated with the intralaminar shear fracture mode. However, the sudden load redistribution caused by the fracture of the 0° plies may have changed the fracture mode depending on the rate sensitivity of the uniaxial fracture stresses (intralaminar shear or transverse tension). Interfaces of adjoining plies with differently oriented fibers but whose fracture surfaces lay within the same depth of field of the SEM could be found. These fracture surface areas often revealed interactions among the plies in that the fracture surface appearances in these small zones could not easily be associated with single fracture modes.

The laminate $[0_2, 90_2]_s$ tested at 45° has plies oriented at either $+45^\circ$ or -45° with respect to the tensile axis. A uniaxial specimen tested at 45° off-axis would have transverse tensile stresses contributing primarily to its fracture (Fig. 9). But with the $+45^\circ$ orientation of the ply, stress calculations indicate that the longitudinal and transverse stresses in all plies are relatively small and intralaminar shear stresses are predominant. In fact, they are predominant over a load angle range between approximately 15° to 75° for an angleplied laminate with this ply configuration. Figure 14 shows the fracture surface of a zero ply from the $[0_2, 90_2]_s$ laminate which was oriented at 45° with respect to the tensile axis. It exhibits the lacerated matrix and clean fiber surfaces typical of the intralaminar shear fracture mode.

From the examples presented and from observations of many other examples not included in this report it was concluded that fracture surface characteristics for a given fracture mode are similar for both uniaxial and angleplied laminates. However, for angleplied laminates no simple load angle range can be associated with a given fracture mode. SEM observations may not be sufficient to identify ranges of fracture modes that occur with various angleplied orientations in MOD I/E composites.

SUMMARY OF RESULTS AND CONCLUSIONS

An investigation into the fracture modes of angleplied high modulus graphite-fiber/epoxy matrix (MOD I/E) composite laminates subjected to off-axis tensile loads revealed the following:

1. The stress-strain curves are linear to fracture.
2. Fracture surface characteristics for a given fracture mode are similar to those for the same fracture mode in uniaxial specimens.
3. At interfaces of plies with fibers oriented at different angles interactions between the plies sometimes result in small zones of fracture surfaces whose fracture modes cannot easily be characterized.
4. Fracture modes in the plies of angleplied laminates can be characterized by SEM observation. Due to adjacent ply interactions, SEM observations may be insufficient to allow association of definite load angle ranges with fracture modes.

REFERENCES

1. J. H. Sinclair and C. C. Chamis, "Fracture Surface Characteristics of Off-Axis Composites," Recent Advances in Engineering Science, Proceedings of the 14th Annual Meeting, Lehigh University, Bethlehem, Pa., G. C. Sih, ed., Society of Engineering Science, 1977, pp. 247-249. (Also NASA TM-73700.)
2. J. H. Sinclair and C. C. Chamis, "Fracture Modes in Off-Axis Composites," Reinforcing the Future; Proceedings of the Thirty-Fourth Annual Conference, New Orleans, La., January 30-February 2, 1979, Society of the Plastics Industry, 1979, pp. 22-A1 to 22-A11. (Also NASA TM-79036, 1979).
3. C. C. Chamis, J. Kring, and T. L. Sullivan, "Automated Testing Data Reduction Computer Program," NASA TM X-68050, 1972.
4. J. H. Sinclair and C. C. Chamis, "Mechanical Behavior and Fracture Characteristics of Off-Axis Fiber Composites. 1 - Experimental Investigation," NASA Technical Paper 1081, 1977.
5. C. C. Chamis and J. H. Sinclair, "Mechanical Behavior and Fracture Characteristics of Off-Axis Fiber Composites. 2 - Theory and Comparisons," NASA TP-1082, 1978.
6. C. C. Chamis, "Computer Code for the Analysis of Multilayered Fiber Composites - Users Manual," NASA TN D-7013, 1971.

TABLE I. - SUMMARY OF MEASURED DATA FROM MODMOR II/EPOXY LAMINATE CENTER GAGE

LOAD ANGLE, deg	FRACTURE STRESS, ksi ^a	FRACTURE STRAIN, %								MODULUS, 10 ⁶ psi ^b				POISSON'S RATIO				COUPLING COEFFICIENT			
		[0 ₂ ±15] _s	[0 ₂ ±30] _s	[0 ₂ ±45] _s	[0 ₂ ±90] _s	[0 ₂ ±15] _s	[0 ₂ ±30] _s	[0 ₂ ±45] _s	[0 ₂ ±90] _s	[0 ₂ ±15] _s	[0 ₂ ±30] _s	[0 ₂ ±45] _s	[0 ₂ ±90] _s	[0 ₂ ±15] _s	[0 ₂ ±30] _s	[0 ₂ ±45] _s	[0 ₂ ±90] _s				
0	68.9	54.7	61.7	53.0	.22	.23	.28	.26	30.9	25.1	22.3	20.5	.79	.2	.86	.07	-0.41	-0.33	0.06	0.10	
10	65.6	48.4	45.5	34.2	.25	.22	.24	.32	26.5	21.5	19.3	11.0	0.70	0.93	0.83	0.35	1.8	-0.44	0.16	1.8	
45	7.5	12.0	24.5	13.4	.22	.21	.22	.50	3.5	5.6	11.0	2.8	0.18	0.29	0.24	0.80	1.3	1.4	0.57	-0.04	
90	4.1	6.3	11.8	51.6	.24	.27	.39	.25	1.2	1.7	2.2	20.5	0.04	0.05	0.31	-0.05	-0.24	0.16	-0.04	0	

^aCONVERSION FACTOR: ksi × 6.8948 = MPa.^bCONVERSION FACTOR: 10⁶ psi × 6.8948 = GPa.

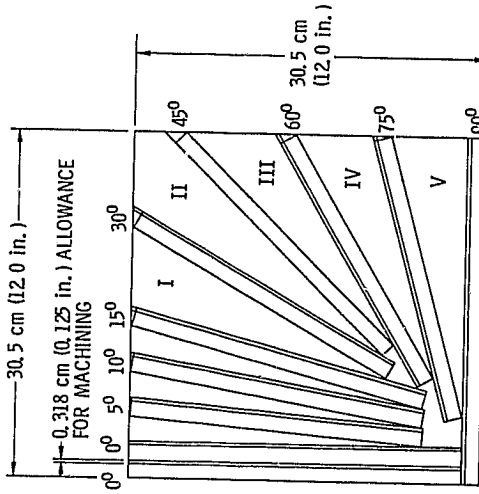
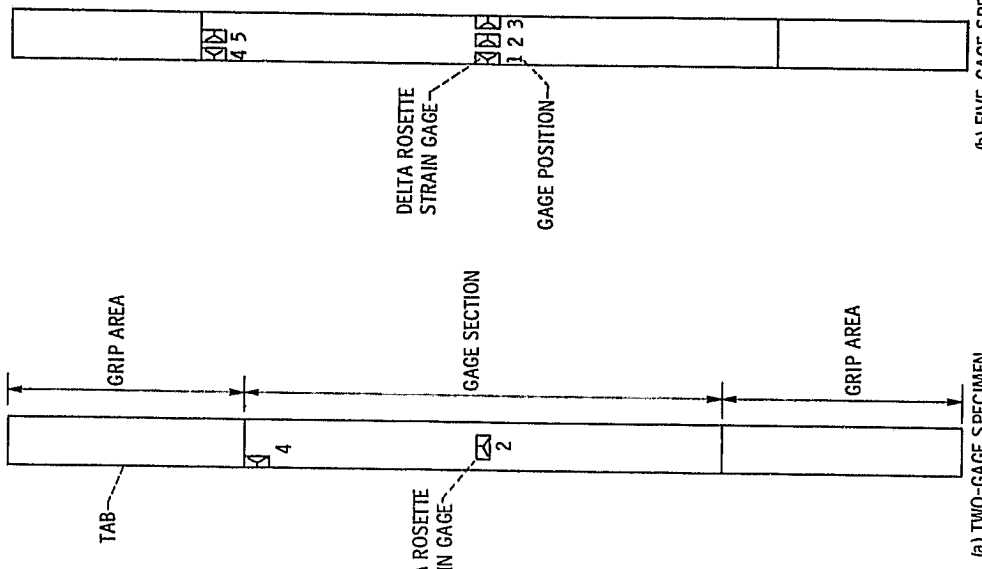


Figure 1. - Specimen layout on Mod I/E composite laminate plate.
CS-77-2374



(a) TWO-GAGE SPECIMEN.



(b) FIVE-GAGE SPECIMEN.
Figure 2. - Schematic of specimen geometry and strain-gage arrangement.
CS-66031

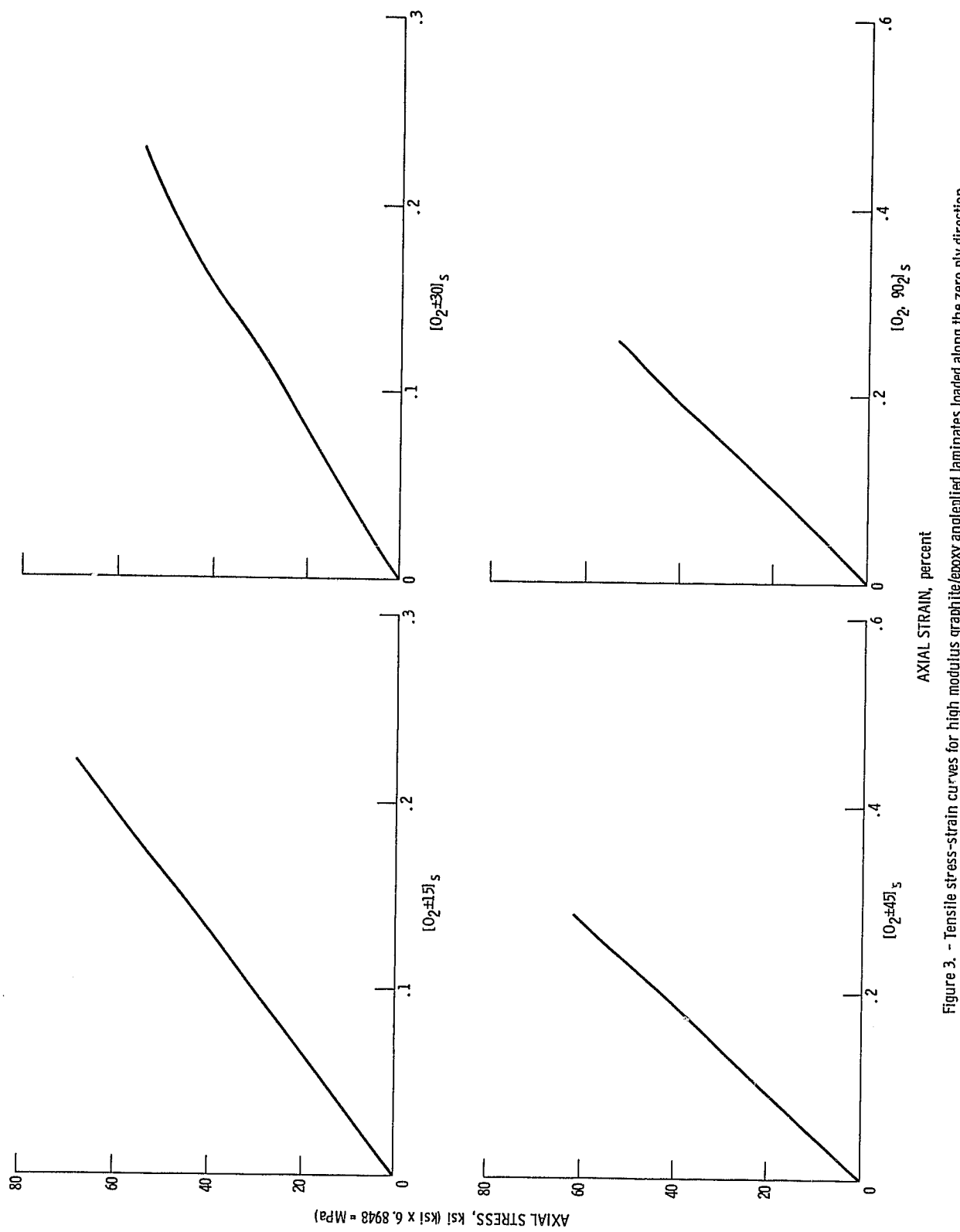


Figure 3. - Tensile stress-strain curves for high modulus graphite/epoxy angleplied laminates loaded along the zero ply direction.

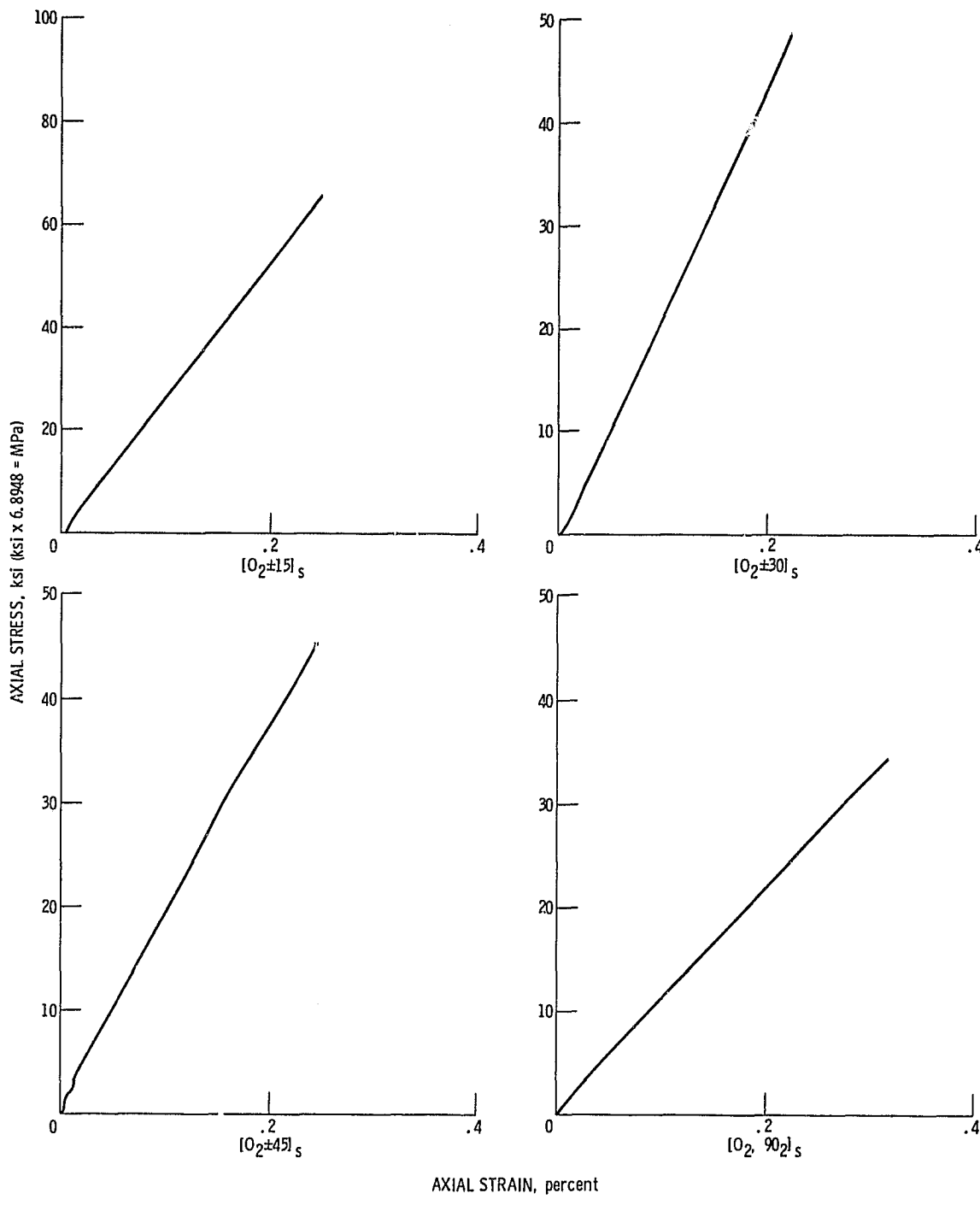


Figure 4. - Tensile stress-strain curves for high modulus graphite/epoxy angleplied laminates loaded 10° off-axis.

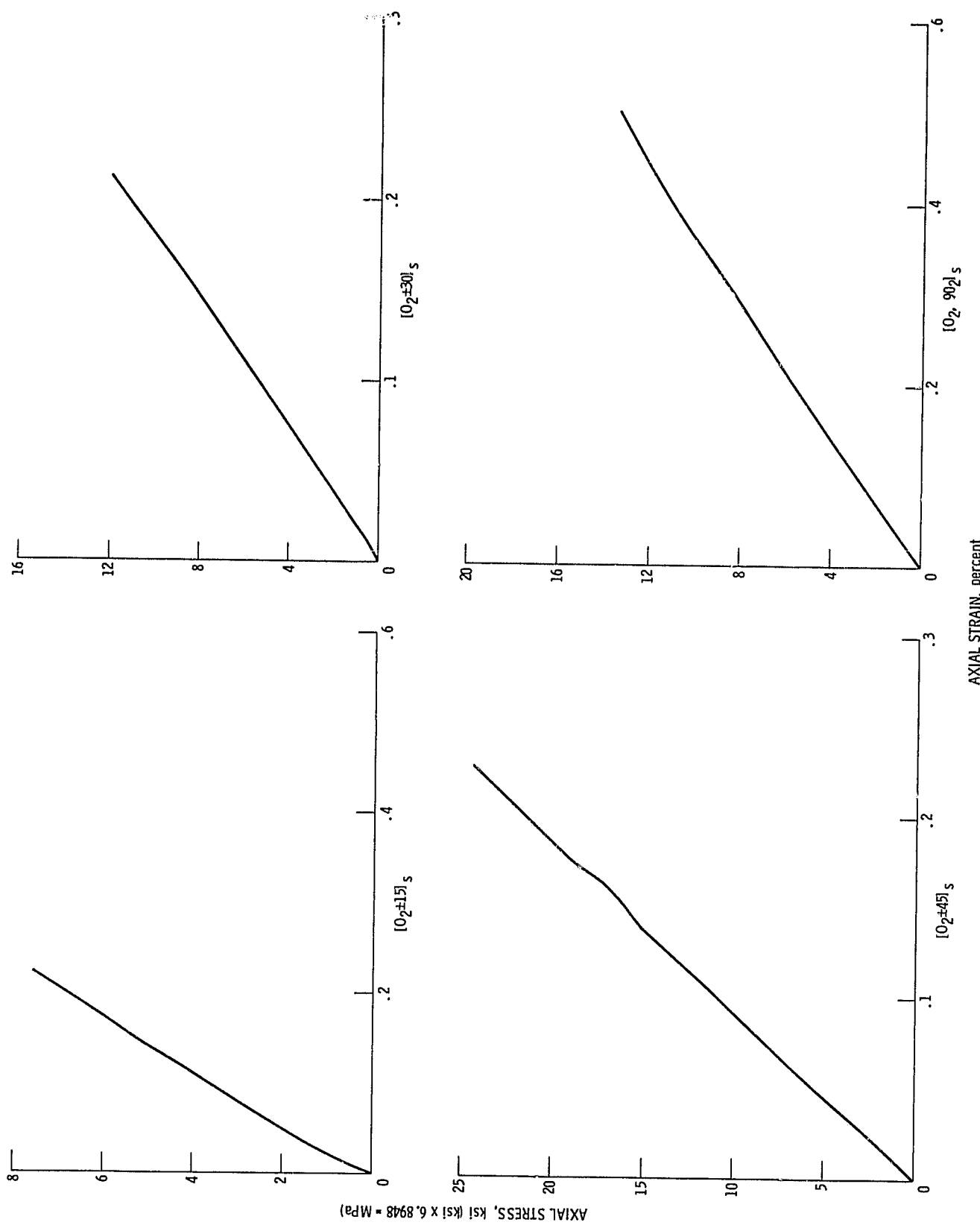


Figure 5. - Tensile stress-strain curves for high modulus graphite/epoxy angleplied laminates loaded 45° off-axis.

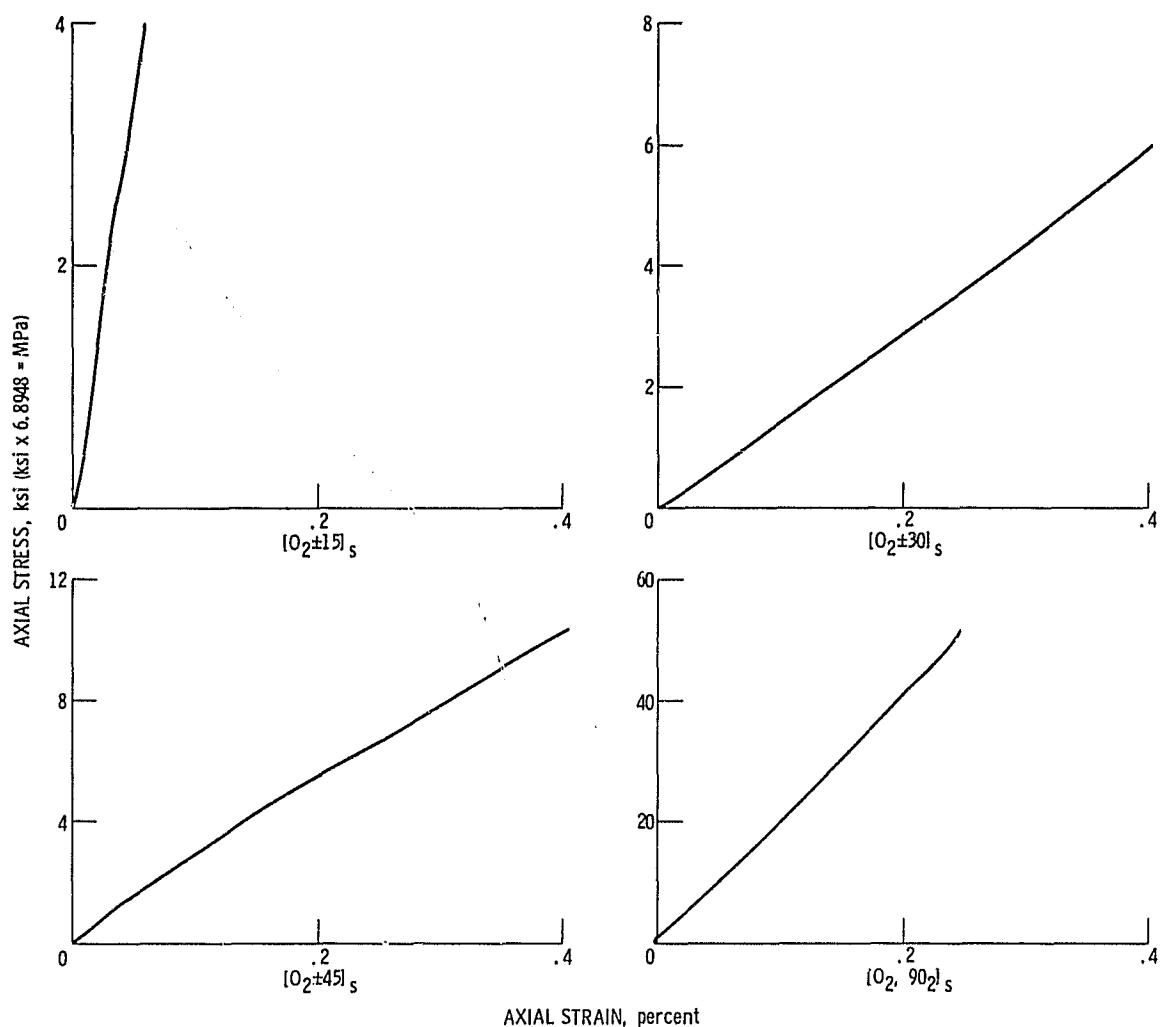


Figure 6. - Tensile stress-strain curves for high modulus graphite/epoxy angleplied laminates loaded 90° to the zero ply direction.

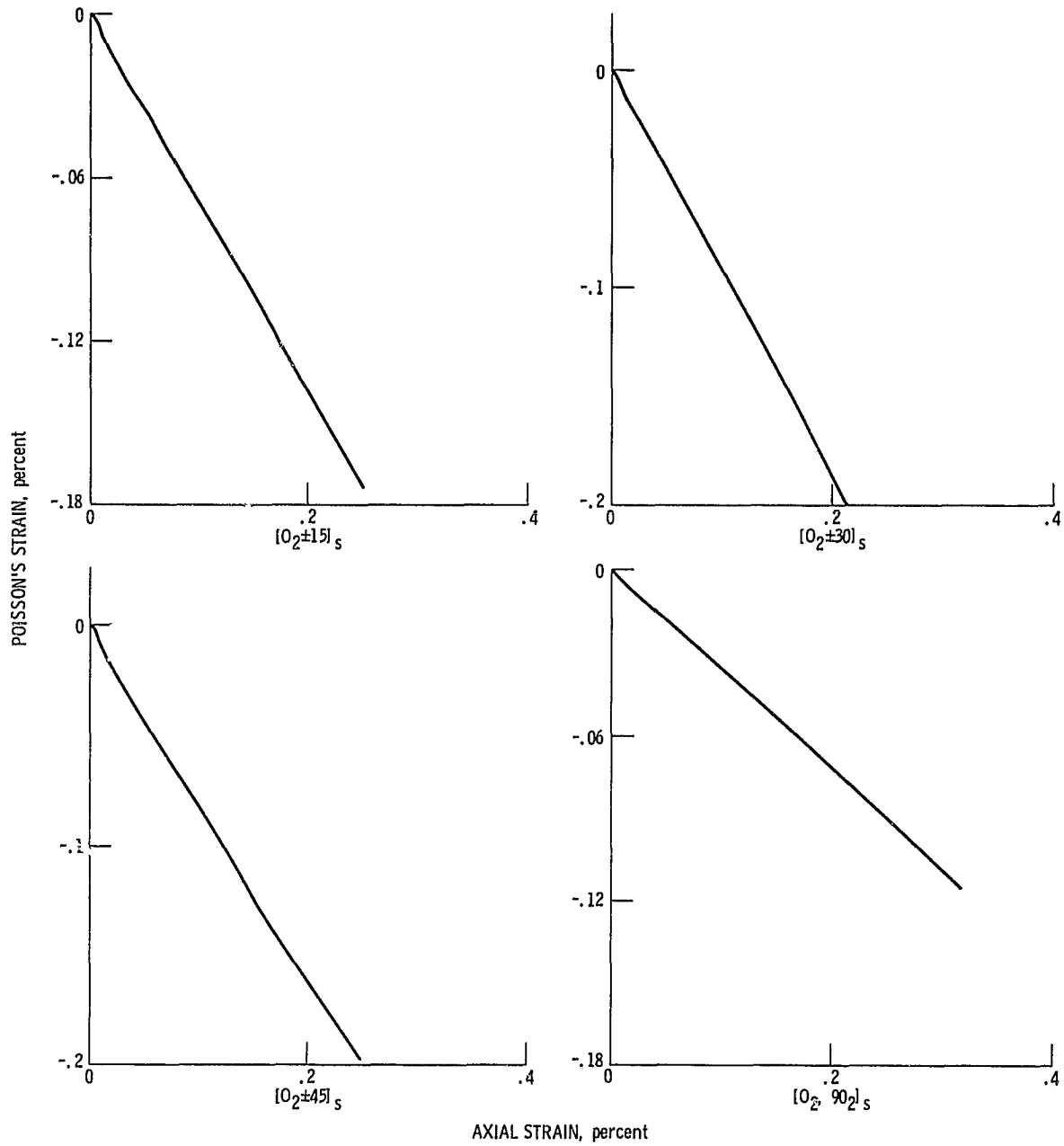


Figure 7. - Poisson's strain curves for high modulus graphite/epoxy angleplied laminates loaded 10° off-axis.

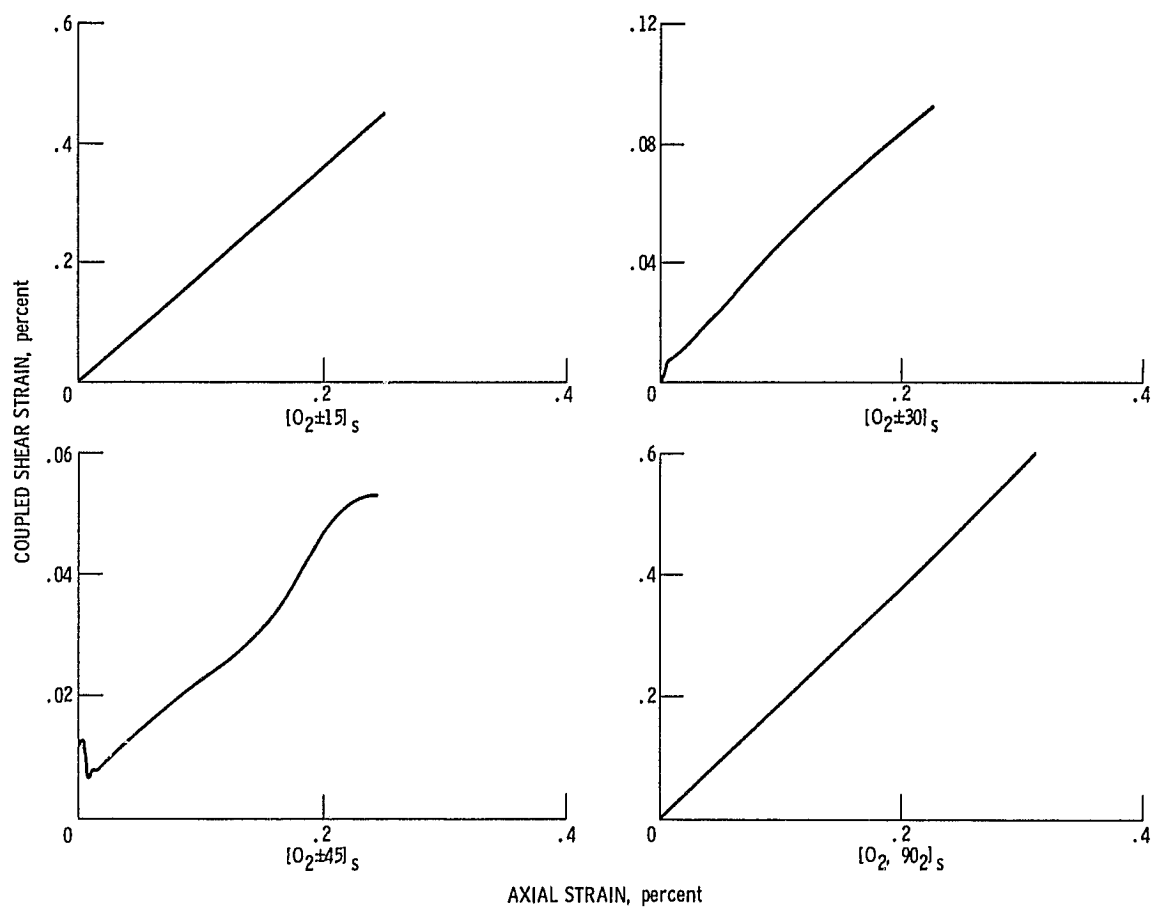


Figure 8. - Coupled shear strain curves for high modulus graphite/epoxy angleplied laminates loaded 10° off-axis.

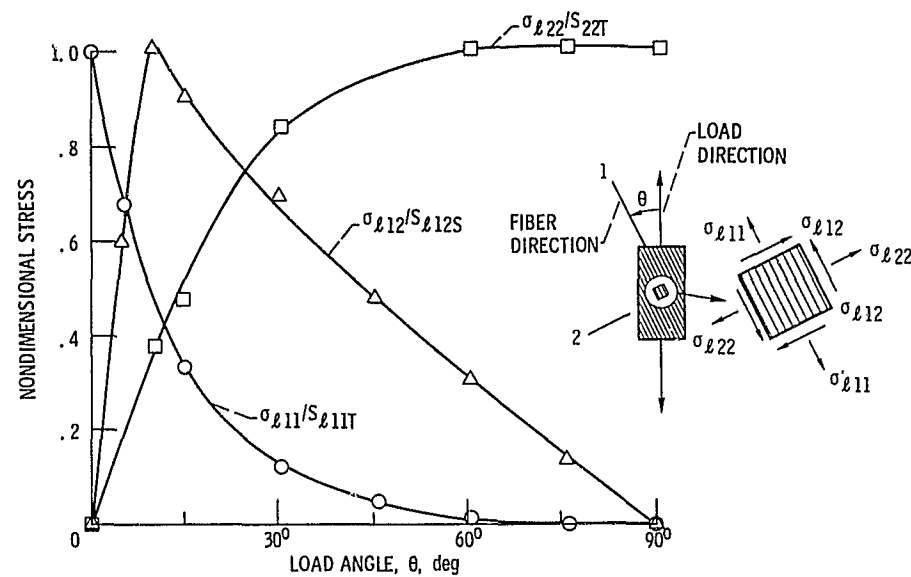


Figure 9. - Fracture stresses normalized with their respective uniaxial strengths.

PLY IDENTIFICATION	[0₂±15]_S			[0₂±30]_S			[0₂±45]_S			[0₂, 90₂]_S		
	0	+θ	-θ	0	+θ	-θ	0	+θ	-θ	0	+θ	-θ
LOAD ANGLE, deg												
0	0	15	-15	0	30	-30	0	45	-45	0	90	90
10	10	25	-5	10	40	-20	10	55	-35	10	-80	-80
30	30	45	15	30	60	0	30	75	-15	30	-60	-60
45	45	60	30	45	75	15	45	90	0	45	-45	-45
90	90	-75	75	90	-60	60	90	-45	45	90	0	0

1 0
 2 0
 3 +θ
 4 -θ
 5 -θ
 6 +θ
 7 0
 8 0

SCHEMATIC OF PLY CONFIGURATIONS

Figure 10. - Ply orientation angles with respect to tensile specimen axes at various loading angles.

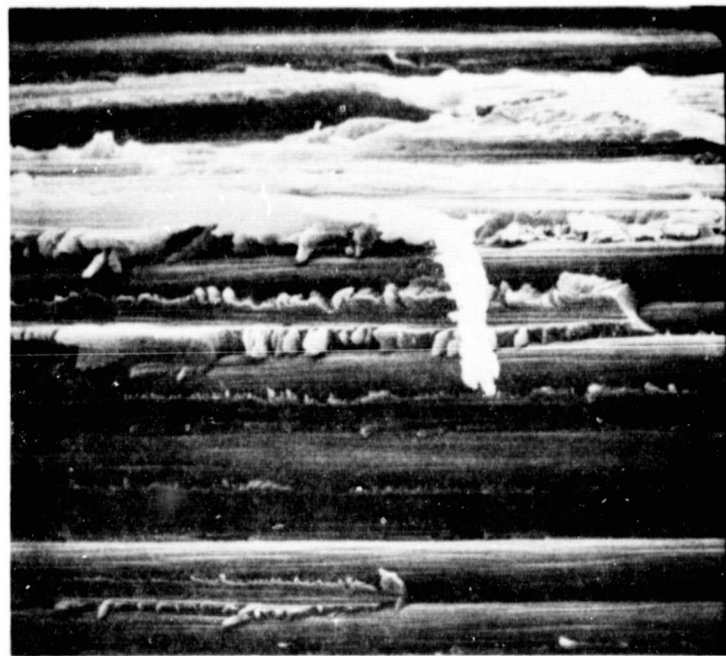
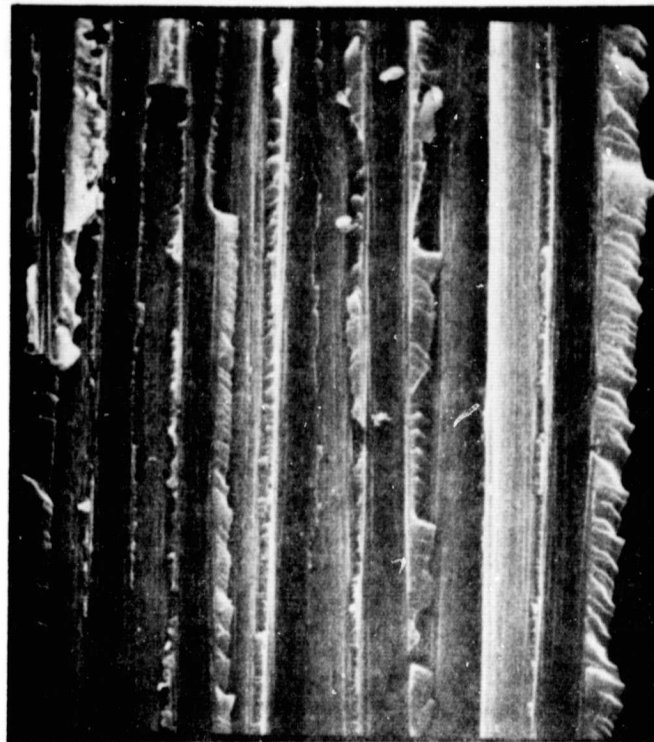
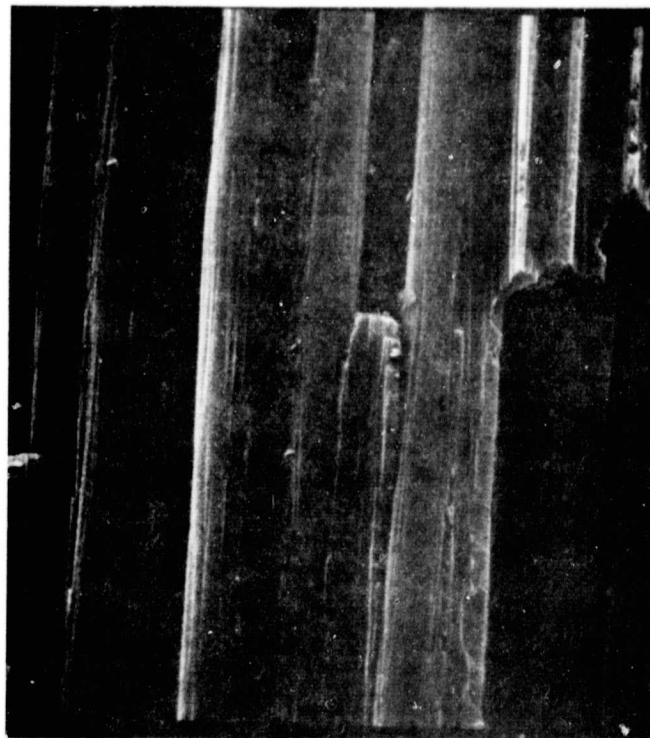


Figure 11. - Fracture surface of 15° ply from $[0_2 \pm 15]_S$ Mod I/E laminate tested along zero ply direction. (Fiber diam: 0.0003 in.)

REPRODUCIBILITY OF THE
ORIGINAL PAGE IS POOR

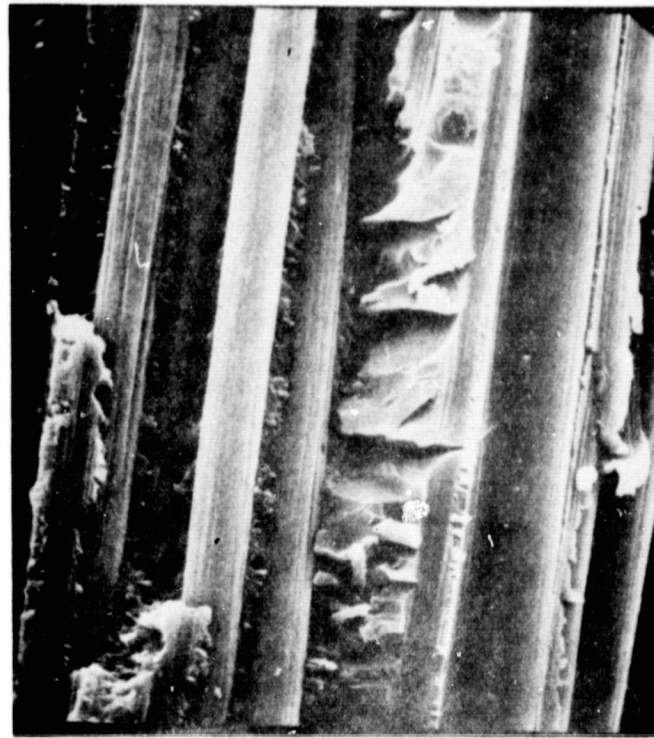


(a) ZERO PLY. FIBERS ORIENTED 30° OFF-AXIS.



(b) +8 PLY. FIBERS ORIENTED 45° OFF-AXIS.

Figure 12. - Fracture surfaces from $[0_2 \pm 15]_S$ Mod I/E laminate tested at 30° off-axis. (Fiber diam: 0.0003 in.)



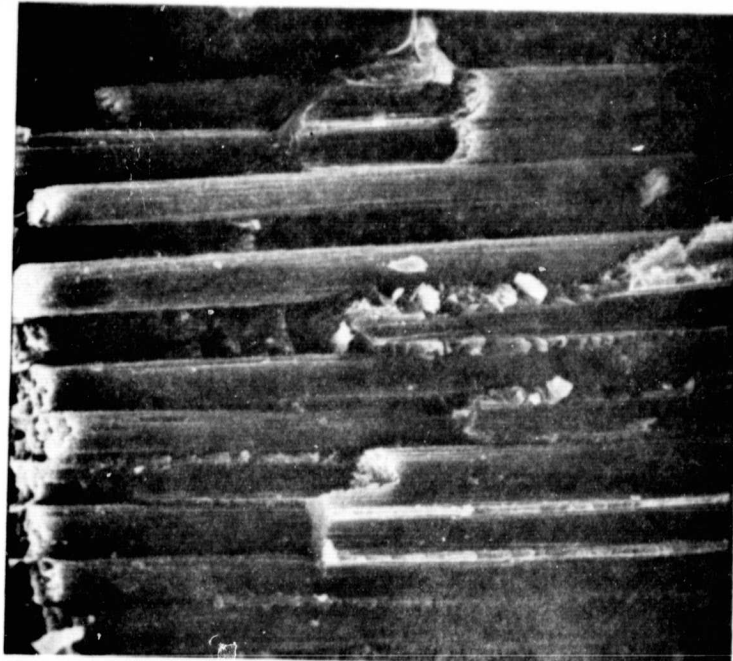
(c) $-\theta$ PLY. FIBERS ORIENTED 15° OFF-AXIS.



(d) GENERAL VIEW. PLY ORIENTATIONS LEFT TO RIGHT: 15° , 45° , 30° OFF-AXIS.

Figure 12. - Concluded.

REPRODUCIBILITY OF THE
ORIGINAL PAGE IS POOR



(a) ZERO PLY. FIBERS ORIENTED 10^0 OFF-AXIS.



(b) $-\theta$ PLY. FIBERS ORIENTED -20^0 OFF-AXIS.

Figure 13. - Fracture surfaces from $[0_2 \pm 30]_S$ Mod I/E laminate tested at 10^0 off-axis.
(Fiber diam: 0.0003 in.)



Figure 14. - Fracture surface of 0° ply from [0 $^{\circ}$ /90 $^{\circ}$] $_s$ Mod I/E laminate tested 45 $^{\circ}$ off-axis. (Fiber diam: 0.0003 in.)

1 Report No NASA TM-81405	2 Government Accession No.	3 Recipient's Catalog No	
4 Title and Subtitle FRACTURE MODES OF HIGH MODULUS GRAPHITE/EPOXY ANGLEPLIED LAMINATES SUBJECTED TO OFF-AXIS TENSILE LOADS		5 Report Date	
7 Author(s) J. H. Sinclair		6 Performing Organization Code	
9. Performing Organization Name and Address National Aeronautics and Space Administration Lewis Research Center Cleveland, Ohio 44135		8. Performing Organization Report No E-319	
12. Sponsoring Agency Name and Address National Aeronautics and Space Administration Washington, D.C. 20546		10. Work Unit No	
		11. Contract or Grant No	
		13. Type of Report and Period Covered Technical Memorandum	
		14. Sponsoring Agency Code	
15. Supplementary Notes			
16. Abstract Angleplied laminates of high modulus graphite fiber/epoxy were studied in several ply configurations at various tensile loading angles to the zero ply direction in order to determine the effects of ply orientations on tensile properties, fracture modes, and fracture surface characteristics of the various plies. It was found that fracture modes in the plies of angleplied laminates can be characterized by scanning electron microscope observation. The characteristics for a given fracture mode are similar to those for the same fracture mode in unidirectional specimens. However, no simple load angle range can be associated with a given fracture mode.			
17. Key Words (Suggested by Author(s)) Angleplied fiber composites; Graphite fibers; Epoxy resin; Mechanical properties; Stress-strain curves; Fracture mode; Testing; Fractographic studies; Matrix laceration		18. Distribution Statement Unclassified - unlimited STAR Category 24	
19. Security Classif. (of this report) Unclassified	20. Security Classif. (of this page) Unclassified	21. No. of Pages	22. Price*

* For sale by the National Technical Information Service, Springfield, Virginia 22161